# Development of a model-based optimal dosage regimen design scheme to minimize paclitaxel and cisplatin induced myelosuppression in non-small cell lung cancer

Yukyung Kim

Department of Medical Science

The Graduate School, Yonsei University

연세대학교
YONSEI UNIVERSITY

# Development of a model-based optimal dosage regimen design scheme to minimize paclitaxel and cisplatin induced myelosuppression in non-small cell lung cancer

Directed by Professor Kyungsoo Park

The Doctoral Dissertation
submitted to the Department of Medical Science,
the Graduate School of Yonsei University
in partial fulfillment of the requirements for the degree of
Doctor of Philosophy

Yukyung Kim

June 2016

연세대학교
YONSEI UNIVERSITY

# This certifies that the Doctoral Dissertation of Yukyung Kim is approved.

---

Thesis Supervisor: Kyungsoo Park

---

Thesis Committee Member #1: Byoung Chul Cho

---

Thesis Committee Member #2: Joo Hyuk Sohn

---

Thesis Committee Member #3: Chung Mo Nam

---

Thesis Committee Member #4: Min Goo Lee

## The Graduate School
## Yonsei University

June 2016

# ACKNOWLEWLEGEMENTS

4년반이라는 길다면 긴 시간 동안 부족한 저를 지도해주시고 조언해주셨고 제가 하고 싶은 것에 대해 지원해주신 저의 지도 교수님, 박경수 교수님께도 머리 숙여 진심 어린 감사 드립니다.

바쁘신 와중에 시간을 내어 논문을 지도해주시고, 아낌없이 조언해주신 조병철 교수님, 손주혁 교수님, 남정모 교수님, 그리고 이민구 교수님께 다시 한번 진심으로 감사를 드립니다. 교수님들의 지도로 지금의 논문이 나올 수 있었습니다. 또한 약리학교실의 큰 기둥이신 김경환 교수님, 열정이 넘치시는 안영수 교수님, 인자하게 약리학교실을 이끌어주시는 김동구 교수님, 폭넓은 식견으로 긴장을 놓지 않게 만들어주신 이민구 교수님, 연구에 힘쓰시는 김철훈, 김주영, 김형범, 지헌영 교수님께도 감사드립니다.

힘든 연구생활동안 들어주고 격려해주고 조언을 아끼지 않았던 약리학교실 선생님들과 저희 임상약리 교실원들에게도 감사드립니다. 특히 저의 동기인 미정이가 아니었으면 끝까지 올 수 없었을 것이기에 특히나 감사하다고 말하고 싶습니다. 교실생활에 도움을 주셨던 임종수 선생님, 민선자 선생님, 김건태 선생님께도 감사드립니다.

마지막으로 무엇보다 남들과 다른 길을 걷겠다는 딸을 반대하지 않고 지켜보시느라 맘고생하신 부모님께 가장 큰 감사를 드립니다.

김유경 드림.

# TABLE OF CONTENTS

# LIST OF FIGURES

# LIST OF TABLES

ABSTRACT

**Development of a model-based optimal dosage regimen design scheme to minimize paclitaxel and cisplatin induced myelosuppression in non-small cell lung cancer**

Yukyung Kim

*Department of Medical Science*

*The Graduate School, Yonsei University*

(Directed by Professor Kyungsoo Park)

Lung cancer is usually discovered after the disease is progressed and chemotherapy plays a major role in the treatment. According to the chemotherapy guideline, a combination therapy with two or more drugs is recommended for advanced stage non-small cell lung cancer (NSCLC) patients. However, a combination therapy can increase not only the effectiveness for the treatment but also the chance of adverse drug reaction (ADR) due to its toxic effect. Myelosuppression is one of the most frequently occurred ADRs during chemotherapy in cancer patients, which can lead to the reduced efficacy of chemotherapy by dose reduction and susceptibility to infection due to reduced neutrophil count. Myelosuppression is known as dose limited toxicity. However, patients treated with a chemotherapy show variable responses in the

currently used BSA-based dosing system. The aim of this study is to develop a model-based optimal dosing scheme to minimize chemotherapy-induced myelosuppression in NSCLC.

Analysis data were retrieved respectively from clinical data retrieve system (CDRS) and electrical medical records (EMR). Included patients were those who were newly diagnosed as stage IIIB or IV NSCLC between January 2009 and December 2013 in Severance hospital, treated with paclitaxel 175 mg/m$^2$ 3hr infusion in day 1 and cisplatin 75 mg/m$^2$ in day 2 as the first line therapy and aged between 18 and 85 yrs old. Patients whose primary tumor was removed by surgery or who were treated with concurrent chemoradiation were excluded. The analysis variable was absolute neutrophil count (ANC) which represents the myelocyte function.

A semi-mechanistic model was used to describe ANC change with time during chemotherapy. A kinetic-pharmacodynamic (K-PD) model incorporating a virtual compartment was used to describe the kinetics of paclitaxel, cisplatin and granulocyte colony stimulating factor (G-CSF) as blood concentration data for these substances were not available. Neutrophil production was described by a single compartment representing proliferative cells, 3 transit compartments representing neutrophil maturation, and a single compartment representing circulating observed blood neutrophils, where neutrophil production was influenced by negative feedback from blood neutrophil count and was assumed to be reduced by chemotherapy.

The final structural model was described as a semi-mechanistic model where combined drug effect for paclitaxel and cisplatin was described by response surface model, and G-CSF effect by an ordinary Emax model. The model shows that $IR_{50,d}$, virtual dose rate of paclitaxel and cisplatin corresponding to 50% of maximum drug inhibition, was reduced by 38% in women, and $KDE_p$, paclitaxel elimination rate from the virtual compartment, was reduced by 85% in patients with DM, which was consistent with the trend observed in raw data. Nevertheless, due to the lack in physiological basis for the relation between these covariates and ANC, more stuides inclusing external validatation would be needed to confirm this finding. Model evaluation based on the precision of parameter estimates, goodness of fit plots and visual predictive check suggested that the proposed model is reasonable and parameter values were estimated with good precision.

Clinically, the proposed model can be used to predict the time to nadir ANC when G-CSF treatment should be involved and to predict how to change dose regimen when it occurs, thereby avoiding serious risk in the immune system caused by severe neutropenia.

---

Key words: neutropenia, quantitative analysis, non-small cell lung cancer, paclitaxel, cisplatin, semi-mechanistic myelosuppression model, kinetic-pharmacodynamic (KPD) model, response surface model, transit compartment model, routine clinical data

# Development of a model-based optimal dosage regimen design scheme to minimize paclitaxel and cisplatin induced myelosuppression in non-small cell lung cancer

YuKyung Kim

Department of Medical Science

The Graduate School, Yonsei University

(Directed by Professor Kyungsoo Park)

## I. INTRODUCTION

Lung cancer is the 4th most frequently occurring cancer in Korean patients and has the highest death rate, 34 dying per a population of 100 thousands according to the Korean Statistical Information Service records in 2013.[1,2] The death rate of lung cancer has not decreased despite advancement in screening tools such as chest X-ray, chest CT, etc. and more than half of lung cancer patients are diagnosed at advanced stage of the disease[3] which might be inoperable. Chemotherapy is one of the important treatment options for patients whose stage is inoperable. Anticancer drugs are commonly used as a combination of two or more drugs acting in different pathways. Because it is expected more effective than monotherapy,[4] a combination therapy is recommended in stage IV non-small cell lung cancer (NSCLC) chemotherapy guideline.[5] However, combination therapy also increases a chance of toxicity.[6] The goal of the chemotherapy of non-small cell lung cancer in advanced stage is improving the survival rate, decreasing symptoms induced by cancer by reducing the tumor size, upgrading the quality of life and minimizing the side effect induced by anticancer treatment.[7] Some side effects like nausea and vomiting could be regulated by the symptom controlling drugs without stopping chemotherapy, but heavy side effects like myelosuppression need to be treated and could delay the chemotherapy cycle or lead to dose reduction that could reduce the efficacy of chemotherapy. Myelosuppression is a frequently occurring adverse event during chemotherapy.[8] Different chemotherapy regimens show the various degree of hematopoietic toxicity.[9,10] Moreover, such toxicity is known to increase as drug exposure is escalated and duration of neutropenia is directly related to a chance of infections.[11] Neutropenia-related infections require aggressive treatment with antibiotics and can be life threatening.[12,13]

There are articles describing myelosuppression induced by chemotherapy. Friberg et al. first described a chemotherapy-induced myelosuppression model explaining hematopoiesis maturation using three kinds of compartments, (i) proliferative cell compartment, (ii) three transit compartments related to cell maturation and (iii) observed blood cell compartment, linked dynamically each other. In this model, chemotherapy agents were modeled to inhibit cell proliferation and then bring about myelosuppression eventually.[14]

Based on this model, a chemotherapy-induced myelosuppression model was further developed to optimize a chemotherapy dose by considering the effect of the covariates,[15-22] to build up a pharmacokinetic-pharmacodynamic (PK-PD) model for combination therapy and find out a predictive marker,[23] to select a dosing regimen,[24,25] to explore the dosing schedules,[26-29] to develop the dosing algorithm not to induce neutropenia[30] and to investigate risk factors related to probability of developing febrile neutropenia.[31] This model was also used to demonstrate granulocyte colony-stimulating factor (G-CSF) effect during anti-cancer therapy.[32,33]

However, all the studies cited above were conducted in the form of a clinical trial, where an overall response could not be evaluated. In addition, most studies were accomplished in western population except for the study conducted in Japanese[18] and the subjects enrolled in the studies had multiple diseases not a single disease.

The objective of this study is to develop a model to describe myelosuppression especially neutropenia when NSCLC patients are treated with combined chemotherapy and to establish an optimal dosage regimen to minimize myelosuppression induced by chemotherapy.

## II. MATERIALS AND METHODS

### 1. Data

The data were retrieved retrospectively from electrical medical records (EMR) of Severance Hospital. The study subjects were screened using clinical data retrieve system (CDRS) and more specific information for the selected patients were collected from EMR.

Total 6058 lung cancer patients treated in Severance hospital between January 2009 and December 2013 were screened using CDRS system. Among them, 327 patients received combination chemotherapy of paclitaxel and cisplatin as first-line treatment, among whom 173 patients satisfied inclusion and exclusion criteria and were included in the analysis. The inclusion criteria were: aged between 18 and 85 yrs old, diagnosed as stage IIIB or IV NSCLC and treated with paclitaxel and cisplatin as the first line chemotherapy. Patients whose primary tumor was removed by surgery or who were treated with concurrent chemoradiation or who were treated with chemotherapy as first-line treatment but were not evaluated for the treatment effect were excluded.

Chemotherapy was scheduled for paclitaxel 175 $mg/m^2$ 3hr infusion on day 1 and cisplatin 75 $mg/m^2$ 3hr infusion on day 2, respectively. The dose was reduced by 25% when grade 4 neutropenia[34] occurred. Dosing continued up to 6 cycles and was stopped when disease progression or condition deterioration occurred. Response evaluation was scheduled after 3 and 6 cycles and whenever disease progression was suspicious. Dependent variable was absolute neutrophil count (ANC) which represented the myelocyte function. ANC was calculated by white blood cell (WBC) count times the percentage of neutrophil divided by 100. The potentially influential covariates information such as demographic factor (height, weight, body surface area (BSA), age when diagnosed, sex, smoking history, disease histories (hypertension(HTN), diabetes mellitus(DM) and pulmonary tuberculosis(Tb)), laboratory data representing hepatic function (aspartate aminotransferase (AST) and alanine transaminase (ALT)) and renal function (serum creatinine, estimated creatinine clearance (CLcr) and estimated glomerular filtration rate (eGFR), where CLcr was calculated using Cockroft-Gault formula[35] and eGFR was estimated using modification of diet in renal disease (MDRD) formula[36,37] and eGFR was automatically reported in order communication system (OCS)) and cancer related information (stage, baseline Eastern Cooperative Oncology Group (ECOG) performance status, baseline tumor size, histology, overall response and performed chemotherapy cycles) were also collected. G-CSF treatment information was collected and incorporated into the model. G-CSF analogues used were filgrastim (Grasin prefilled injection®, Leukokine injection® and Leucostim injection®) and lenograstim (Neutrogin injection®), and were treated the same as G-CSF.

For most of the ANC data, two samples were collected before and after the chemotherapy in each cycle, with additional samples collected when the G-CSF treatment was added. Weight, BSA and laboratory test information were allowed to change in each cycle. If the patient covariate information was missing, it was substituted by the information from the previous sampling time or by the mean value of pervious and next times.

## 2. Model development

### A. A semi-mechanistic myelosuppression model

The PD was described as a semi-mechanistic model proposed by Friberg et al.[14] The structural model was composed of a single compartment representing stem cells and progenitor cells, i.e., proliferative cells [*Prol*], three transit compartments representing maturing cells [*Transit*], and a single compartment representing circulating observed blood cells [*Circ*]. A maturation chain, represented by transit compartments and associated rate constant (*Ktr*), allowed prediction of a time delay between drug administration and an observed effect. The generation of new cells in Prol was dependent on the number of cells in the compartment, that is, self-renewal or mitosis, a proliferation rate constant determining the rate of cell division (*Kprol*), and a feedback mechanism from the circulating cells $(Circ_0/Circ)^{\gamma}$. The feedback function is governed by the $\gamma$ parameter, which reflects the increase in self-replication rate occurring when circulating cells are depleted. The feedback loop was necessary to describe the rebound of cells, i.e., an overshoot compared with the baseline value [$Circ_0$]. Under the presence of drug ($E_d$) and G-CSF effects ($E_G$), the differential equations were written as:

$$\frac{\mathrm{dProl}}{\mathrm{dt}} = Kprol * Prol * (1 - E_d) * (1 + E_G) * \left(\frac{Circ_0}{Circ}\right)^{\gamma} - \mathrm{Ktr} * \mathrm{Prol} \tag{1}$$

$$\frac{\mathrm{dTransit1}}{\mathrm{dt}} = Ktr * Prol - Ktr * Transit1 \tag{2}$$

$$\frac{\mathrm{dTransit2}}{\mathrm{dt}} = Ktr * Transit1 - Ktr * Transit2 \tag{3}$$

$$\frac{\mathrm{dTransit3}}{\mathrm{dt}} = Ktr * Transit2 - Ktr * Transit3 \tag{4}$$

$$\frac{\mathrm{dCirc}}{\mathrm{dt}} = Ktr * Transit3 - Kcirc * Circ \tag{5}$$

$$Ktr = Ktr_0 * (1 + E_G) \tag{6}$$

where $Ktr_0$ is pre-treatment value of *Ktr* evaluated at $E_G = 0$.

In the transit compartments, it is assumed that only loss of cells is into the next compartment. Although the work cited above selected three transit compartments, other number of compartments was tested. As the proliferative cells differentiate into more mature cell types, the concentration of cells is maintained by cell division. Basic assumption for the model is that, at steady state, *dProl/dt = 0*, and therefore *Kprol* = *Ktr*. To minimize the number of parameters to be estimated, it was assumed in the modeling that *Kcirc* = *Ktr*. To improve interpretability, mean transit time (*MTT*) was estimated instead of *Ktr*. *Ktr* was expressed by (number of compartment *(n)* + 1) divided by *MTT.*

**B. A kinetic-pharmacodynamic (KPD) drug model**

The blood concentrations of chemotherapy and G-CSF were not available in this study. Therefore, a KPD model based on a hypothetical compartment[38,39] and virtual drug kinetics was used.

In detail, the kinetics of each of the two anticancer drugs and the G-CSF was characterized by a virtual one-compartment model (aimed to represent the biophase) with bolus input as follows.

$$\frac{\mathrm{d}A_d}{\mathrm{dt}} = -KDE_d * A_d \tag{7}$$

$$VIR_d = KDE_d * A_d \tag{8}$$

where $A_d$ represents the amount of drug in the hypothetical compartment, $KDE_d$ the elimination rate constant from the virtual compartment which corresponded to $K_{e0}$ in the effect compartment model and $VIR_d$ the virtual infusion rate of drug distributed into PD sites.

### C. Drug effect of combination therapy

Drug effect of paclitaxel and cisplatin was described either empirical additive model expressed by log linear function (Eq. (9)) or response surface model developed by Minto et al. (Eq. (10)).[40] Then, *VIR* was substituted into these models as below.

$$E_d = e^{(-Scale1*VIR_P - Scale2*VIR_C)} \tag{9}$$

$$E_d = \frac{\left(\frac{\left(\frac{VIR_P}{IR_{50}} + \frac{VIR_C}{IR_{50}}\right)}{U_{50}}\right)^{\gamma}}{1 + \left(\frac{\left(\frac{VIR_P}{IR_{50}} + \frac{VIR_C}{IR_{50}}\right)}{U_{50}}\right)^{\gamma}} \tag{10}$$

where *Scale* represents the slope related to the dose-driving rate and the drug effect, $E_d$. $IR_{50}$ represents *VIR* associated with 50% of maximum effect and $U_{50}$ is the number of units associated with 50% of maximum drug effect at the given ratio of drug combination and $\gamma$ is the steepness of the concentration-response relation at given ratio of drug combination. Developed to describe pharmacodynamic interactions of drugs, response surface model can assess the type (additive, synergistic, or antagonistic) and severity of drug-drug interaction in combination therapy.

### D. G-CSF effect

Previous articles did not consider the effect of G-CSF treatment other than Ramon-Lopez et al.,[39] where the G-CSF effect was incorporated into the mean transit time (*MTT*) and *Kprol* as a time-dependent dichotomous covariate as in Eq. (11) because G-CSF shortened the *MTT* and increased the mitotic activity.[39,41]

$$P^* = P_0 \times (1 + \theta_p \times GCSF) \tag{11}$$

where $P^*$ was a typical value of each parameter of *Ktr* and *Kprol*, which was $P_0$ in the absence of G-CSF or $P_0 \times (1 + \theta_p)$ in the presence of G-CSF, respectively. $\theta_p$ quantified the relative contribution of the G-CSF effect to each parameter, with *GCSF* being an indicator variable denoting the value of 1 for the G-CSF treatment and 0 otherwise.

In this work, however, considering that G-CSF affected myelocyte continuously, KPD model strategy was also used. Then, G-CSF effect was described as either the linear (Eq. (14)) or the ordinary Emax model (Eq. (15)). G-CSF effect was incorporated into *Ktr* (Eq. (16)) and the proliferation compartment.

$$\frac{\mathrm{d}A_G}{\mathrm{dt}} = -KDE_G * A_G \tag{12}$$

$$VIR_G = KDE_G * A_G \tag{13}$$

$$E_G = 1 + Scale3 * VIR_G \tag{14}$$

$$E_G = 1 + (VIR_G/(VIR_G + IR_{50,G}) \tag{15}$$

$$Ktr = \frac{n+1}{MTT} * E_G \tag{16}$$

**E. Model assumption**

The drug concentration data for paclitaxel and cisplatin was not available in this study, causing numerical difficulty with estimating model parameters with reasonable precision. Therefore, the model was simplified using several assumptions including

$U_{50}$ and γ fixed at 1 so that the 2 drugs were assumed to be additive. Thus, in the case of the response surface model, parameters to be estimated were $Circ_0$, *MTT* and *γ* for system-related model parameters, $IR_{50}$ and *KDE* for paclitaxel ($KDE_p$) and cisplatin ($KDE_c$) for drug-specific parameters and $KDE_G$ and $IR_{50,G}$ for G-CSF specific parameters.

## F. Covariate selection

After the basic model for drug and G-CSF effects was selected, covariates that would have significant influence on model parameters were searched using stepwise covariate modeling (SCM) procedure with significance level of $P \leq 0.01$ for the forward inclusion and $P \leq 0.001$ for the backward deletion. In doing so, the difference in objective function values (OFV) between two nested models (i.e., the models with and without a covariate) was assumed to be approximately $\chi^2$-distributed, with the OFV difference of 3.84 at 1 degree of freedom (d.f.) corresponding to significance level of $P = 0.05$. Covariates tested included BSA, ALT, CLcr or eGFR, sex, age, HTN, DM, Tbc, smoking history, and ECOG performance status.

## G. Statistical model

For statistical model building, an exponential error model was used to model for interindividual variability (IIV) assumed to be normally distributed with mean zero and variance $\omega^2$. For residual unexplained variability (RUV) assumed to be normally distributed with mean zero and variance $\sigma^2$, combined error models were used. To reduce the number of parameters to be estimated, the IIV was incorporated in only part of model parameters. For example, in the case of the response surface model, it was included in $Circ_0$, *MTT*, $IR_{50}$ and *KDE* only, where the IIV of $IR_{50}$ and *KDE* were assumed to be the same for the 2 drugs.

## 3. Model Evaluation

Model selection at each step was done based on Akaike information criterion (AIC). Then, the selected model was evaluated based on goodness-of-fit (GOF) plots, precisions of model parameter estimates, and visual predictive checks (VPC) using 1,000 datasets simulated from the final model.

## 4. Software

All analyses were conducted using NONMEM version 7.3 (ICON Development solutions, Ellicott City, MD, USA)[42] and the first order conditional estimation with interaction (FOCE inter) method was used for model building. PsN version 4.2 was used for SCM.[43,44] Model diagnostics of goodness of fit and visual predictive check plots were produced using PsN and R program version 3.2.1.

# III. RESULTS

## 1. Data

A total of 1686 ANC observations collected from 828 cycles of combination chemotherapy given to 173 patients were recorded, indicating approximately 2 ANC samples were taken each cycle. The mean of the baseline ANC was $5.5\times10^9$ cells/L. G-CSF treatments were given 63 times to 37 patients whenever grade 4 neutropenia was reported. Detailed information for the subjects' characteristics was shown in **Table 1**.

**Table 1. Patient baseline characteristics**

**(a) Continuous characteristics**

| | Mean (SD) | Median (Min-Max) |
|---|---|---|
| **Age (yrs)** | 61.0 (9.2) | 62 (38-82) |
| **Weight (kg)** | 63.5 (11.3) | 63 (38-107) |
| **Height (cm)** | 164.3 (8.6) | 165 (140-186) |
| **BSA ($m^2$)** | 1.7 (0.2) | 1.7 (1.2-2.3) |
| **ALT (IU/L)** | 21.1 (19.3) | 16 (6-187) |
| **AST (IU/L)** | 22.7 (19.9) | 18 (9-190) |
| **Creatinine (mg/dL)** | 0.9 (0.2) | 0.85 (0.40-1.59) |
| **cCLcr (mL/min)** | 80.9 (24.5) | 76 (37-182) |
| **eGFR (mL/min/1.73 $m^2$)** | 85.7 (15.3) | 89 (46-133) |
| **T. bilirubin (mg/dL)** | 0.5 (0.2) | 0.5 (0.1-1.4) |
| **White bllod cells ($x10^9$ cells/L)** | 8.3 (2.6) | 7.9 (2.1-20.6) |
| **Baseline absolute neutrophil counts ($x10^9$ cells/L)** | 5.5 (2.3) | 5.2 (0.9-17.1) |
| **Primary tumor size (cm) n= 145** | 4.7 (2.3) | 4.3 (0.9-17.0) |

**(b) Categorical characteristics**

| | | | |
|---|---|---|---|
| **Sex, n (%)** | | **G-CSF treatment, n (%)** | |
| Men | 127 (73.4) | No | 136 (78.6) |
| Women | 46 (26.6) | Yes | 37 (21.4) |
| **ECOG Performance status, n (%)** | | **Overall response, n (%)** | |
| 0 | 149 (86.1) | PR | 45 (26) |
| 1 | 24 (13.9) | SD | 55 (31.8) |
| **Stage, n (%)** | | PD | 73 (42.2) |
| IIIB | 43 (24.9) | **HTN, n (%)** | |
| IV | 130 (75.1) | No | 88 (50.9) |
| **Histology, n (%)** | | Yes | 85 (49.1) |
| Adenoca. | 119 (68.8) | **DM, n (%)** | |
| Squamous cell ca. | 50 (28.9) | No | 141 (81.5) |
| Unspecified | 4 (2.3) | Yes | 32 (18.5) |
| **Treated cycles, n (%)** | | **Pulmonary Tbc, n (%)** | |
| 2 | 8 (4.6) | No | 152 (87.9) |
| 3 | 37 (21.4) | Yes | 21 (12.1) |
| 4 | 27 (15.6) | **Smoker, n (%)** | |
| 5 | 12 (6.9) | Non | 51 (29.5) |
| 6 | 89 (51.4) | Current | 72 (41.6) |
| | | Ex | 50 (28.9) |

## 2. Model development

### A. Basic model for drug effect

At the beginning, analysis was evaluated using the data of 136 patients who were not treated with G-CSF. For the semi-mechanistic model, analysis was conducted with the model with 1 to 3 transit compartments. For the KPD drug models, the kinetics expressed by the virtual compartment were tested. For the combination effect of the drugs, response surface model assumed that $IR_{50}$ or *KDE* of paclitaxel and cisplatin was the same. Additive model was also tested for the combination drug effect. **Table 2** shows the OFV of the models to be tested.

**Table 2. Basic model for drug effect (n = 136)** ; patients receiving G-CSF excluded

| | # of transit compartment | OFV | AIC | # of Parameters |
|---|---|---|---|---|
| **KPD models** | | | | |
| **Response surface model** | | | | |
| | 3 | 1979.41 | 2003.41 | 12 |
| IR50P=IR50C* | 2 | 1995.14 | 2019.14 | 12 |
| | 1 | not estimated | | |
| | 3 | 1970.21 | 1994.21 | 12 |
| KDEP=KDEC* | 2 | 1970.98 | 1994.98 | 12 |
| | 1 | 2025.06 | 2049.06 | 12 |
| **Additive model expressed by log linear model** | | | | |
| IR50P=IR50C* | 3 | not estimated | | |
| KDEP=KDEC* | 3 | not estimated | | |

* IR50P: $IR_{50,p}$, IR50C: $IR_{50,c}$, KDEP: $KDE_p$ and KDEC: $KDE_c$

As shown in **Table 2**, the drug combination models with additive form were not estimated, apparently because additive form itself was not identifiable for this model because both paclitaxel and cisplatin inhibit ANC production in the proliferation compartment. The response surface models which assumed that *KDE* of paclitaxel and cisplatin was the same ($KDE_p$=$KDE_c$) showed lower AIC, but the estimate of

$ID_{50,p}$ was unreasonably large and the parameter precision was not attainable. On the other hand, the model assuming that $IR_{50}$ of paclitaxel and cisplatin was the same ($IR_{50,p}$ = $IR_{50,c}$) showed better parameter precision and reasonable parameters estimates, probably because paclitaxel and cisplatin doses were administered almost at the same time and could not distinguish each maximum effect, and therefore assuming $IR_{50}$ to be the same resulted in the model more stabilized. Between the models assuming $IR_{50,p} = IR_{50,c}$, the model with three transit compartments showed the lowest AIC, as in Friberg's article.[14]

### B. Basic model for drug and G-CSF effects

The basic model selected for drug effect using 136 subjects' data was used as a template to build the basic model for the entire dataset consisting of 173 patients among whom 37 received G-CSF treatment. To this end, several types of G-CSF models were tested, as shown in **Table 3**.

**Table 3. Basic model for the entire dataset (n = 173)**

**(a) Basic model with drug effect**

| | **OFV** | **AIC** | **no. of parameters** |
|---|---|---|---|
| | 2997.67 | 3021.67 | 12 |

**(b) Basic model with drug and G-CSF effects**

| | **OFV** | **AIC** | **no. of parameters** |
|---|---|---|---|
| **Treated as covariate** | 2817.18 | 2845.18 | 14 |
| **KPD models** | | | |
| **Linear model** | not estimable | | |
| **Ordinary Emax model** | | | |
| **Interindividual variability (IIV) on:** | | | |
| $Circ_0$, MTT, $IR_{50}$, KDE, $IR_{50,G\text{-}CSF}$, $KDE_{G\text{-}CSF}$ | 2904.60 | 2936.60 | 16 |
| $Circ_0$, MTT, $IR_{50}$, KDE, $KDE_{G\text{-}CSF}$ | 2906.33 | 2936.33 | 15 |
| $Circ_0$, MTT, $IR_{50}$, KDE, $IR_{50,G\text{-}CSF}$ | 2904.52 | 2934.52 | 15 |
| $Circ_0$, MTT, $IR_{50}$, KDE | 2906.21 | 2934.21 | 14 |

The model treating G-CSF effect as a covariate showed lowest AIC and reasonably well estimated parameter values. However, as mentioned in the method section, the ANC response following G-CSF injection was a continuous process and the use of the KPD model would be useful to describe the G-CSF effect. The linear KPD model was not estimable, with parameter precision being very poor, probably because the linear model explained only limited effect for this study. In contrast, the ordinary Emax model driven by virtual infusion rate displayed the reasonable parameter estimates and precision. The IIVs related to G-CSF parameters ($IR_{50,G}$ and $KDE_G$) were excluded because of poor precision, and OFV was not significantly increased after removing these IIVs. This was probably because G-CSF information was not enough to estimate the IIV or the number of subjects treated with G-CSF was insufficient for precise estimation. Nevertheless, the model with the G-CSF effect showed significantly less objective function values (OFV) than the model without the G-CSF effect ($\Delta$OFV = -91.46, d.f. = 2, $P < 0.0001$). Final model structure was displayed in **Figure 1**.

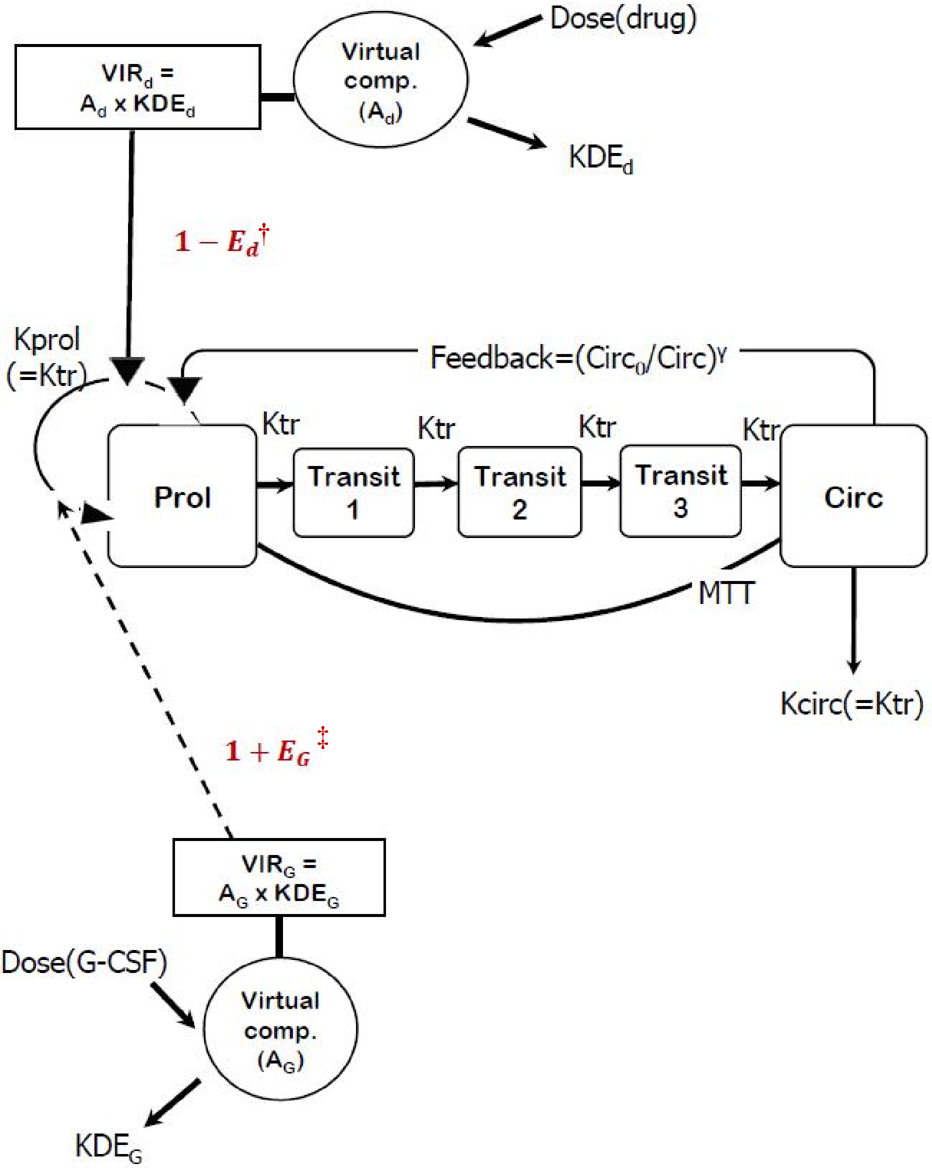


**Figure 1. Schematic representation of the final model.**

†$E_d = (VIR_P/IR_{50,d} + VIR_C/IR_{50,d}) \,/\, \{1 + (VIR_P/IR_{50,d} + VIR_C/IR_{50,d})\}$

‡$E_G = VIR_G \,/\, (VIR_G + IR_{50,G})$

### C. Covariate selection

In the covariate selection step, sex was incorporated into $IR_{50,d}$ and DM into $KDE_p$, yielding a significant improvement in model fit as compared to basic model. Covariate selection step was represented in **Table 4**.

**Table 4. Covariate selection step (Forward selection)**

| | Covariate | $OFV_{OLD}$ | $OFV_{NEW}$ | ΔOFV | Criterion | d.f. | P-value |
|---|---|---|---|---|---|---|---|
| Step 1 | SEX on $IR_{50,d}$ | 2906.21 | 2878.92 | -27.29 | < -6.63 | 1 | $1.8 \times 10^{-7}$ |
| Step 2 | DM on $KDE_p$ | 2878.92 | 2861.40 | -17.52 | < -6.63 | 1 | $2.8 \times 10^{-5}$ |

$IR_{50,d}$ and $KDE_p$ : $IR_{50}$ of paclitaxel and cisplatin and *KDE* of paclitaxel

$OFV_{OLD}$ : OFV before covariate is added

$OFV_{NEW}$ : OFV after covariate is added

d.f.: Degree of freedom

The final estimates of model parameters were presented in **Table 5**. This result shows that $IR_{50,d}$, virtual dose rate corresponding to 50% of maximum drug inhibition, was reduced by 38% in women, and $KDE_p$, paclitaxel elimination rate constant from the virtual compartment, was reduced by 85% in DM. The precision of the NONMEM parameter estimates was acceptable as presented in **Table 5,** which showed that the relative standard error (RSE) was lower than 44% except for $IR_{50,G}$. This is probably because data points were not sufficient enough to estimate maximum effect for G-CSF. Nevertheless, all the parameters except for $IR_{50,G}$ showed relatively good precision.

**Table 5. Final model parameter estimates**

| Model parameters | Parameter estimates (%RSE) | Shrinkage, % |
|---|---|---|
| **Structural model** | | |
| $Circ_0$ ($x10^9$/L) | 5.25 (2.8) | |
| MTT (Days) | 4.65 (3.4) | |
| $\gamma$ | 0.174 (4.9) | |
| $IR_{50,d}$ (mg/day) | 105 (6.2) | |
| $KDE_p$ (/day) | 0.0427 (12.0) | |
| $KDE_c$ (/day) | 0.279 (19.4) | |
| $IR_{50,G}$ (mcg/day) | 65.5 (61.9) | |
| $KDE_G$ (/day) | 6.84 (41.7) | |
| **Covariate effects (%)** | | |
| $IR_{50,d}$ in woman | -0.383 (14.5) | |
| $KDE_p$ in DM | -0.850 (5.6) | |
| **Interindividual Variability** | | |
| $\omega$ ($Circ_0$) | 22.7 (10.7) | 0.1964 |
| $\omega$ (MTT) | 20.1 (11.3) | 0.2736 |
| $\omega$ ($IR_{50,d}$) | 30.6 (16.0) | 0.3566 |
| $\omega$ ($KDE_d$) | 79.3 (12.6) | 0.3442 |
| **Residual Variability** | | |
| $\sigma_{proportional}$ (%CV) | 33.1 (2.9) | |
| $\sigma_{additive}$ ($x10^9$/L) | 0.466 (10.8) | |

Goodness of fit plots in **Figure 2** showed scatter plots centered around the identity line except few points, indicating that the established model did well describe the data. The few points out of the identity line were related to G-CSF treatment. It was assumed that predicted ANC was estimated slightly higher than observed ANC after G-CSF treatment. The visual predictive check plot in **Figure 3** showed that the observed ANC concentrations were well described by the predicted ANC concentration. These findings supported a reasonable accuracy and precision of the NONMEM parameter estimates.

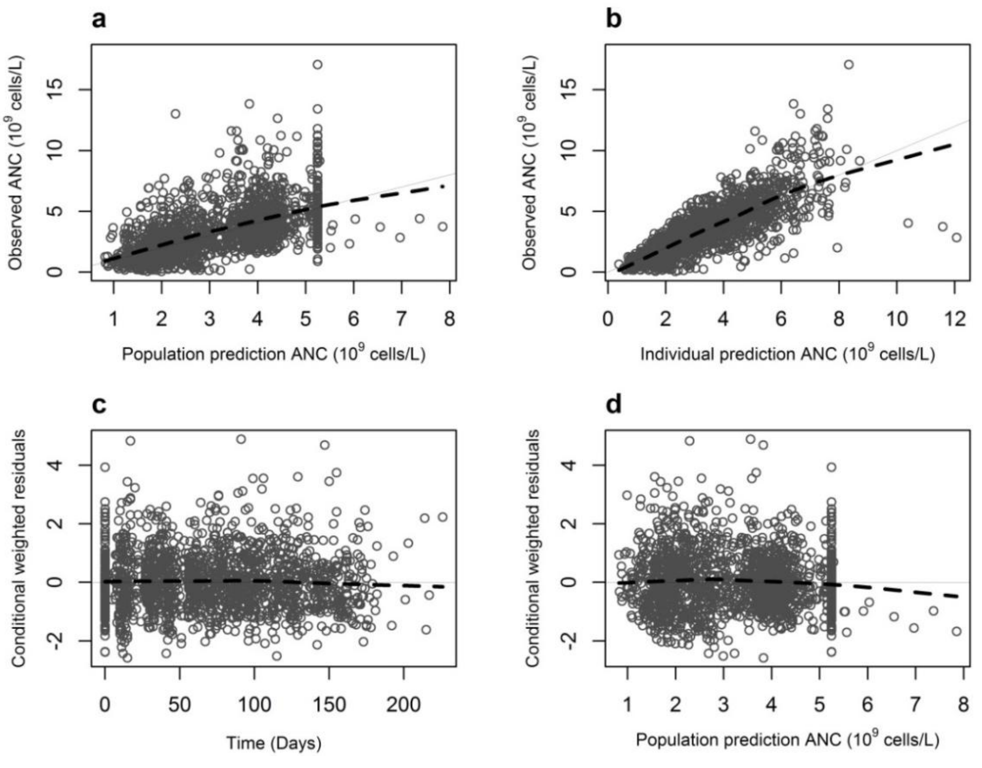


**Figure 2**. **Goodness of fit plot of the final model. a**. ANC vs. population model predictions, **b**. ANC vs. individual model predictions, **c**. The conditional weighted residuals vs. time and **d**. The conditional weighted residuals vs. population model predictions. The circles represented the observations, the grey thin line represented the line of identity and the black dashed line represented the smoother line.

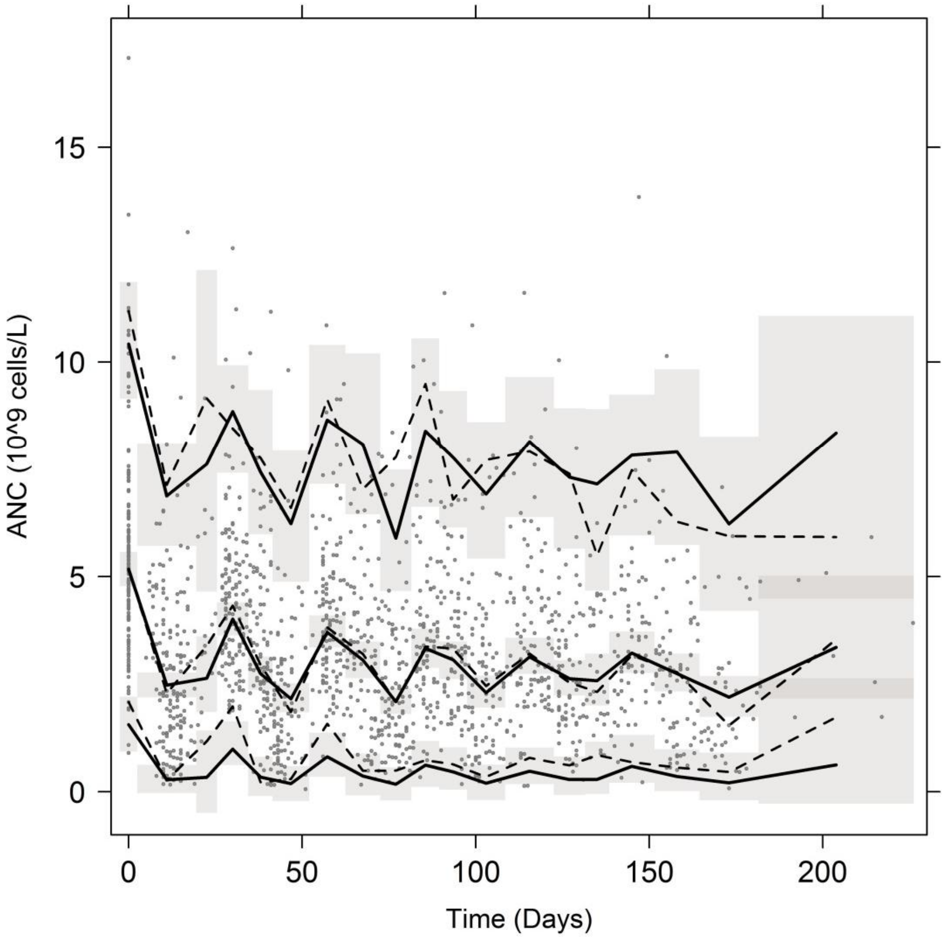


**Figure 3**. **VPC plot of the final model.** The observed data (*dark blue circles*) were plotted with the 2.5th, 50th and 97.5th percentiles (*black dashed lines*) and 2.5th, 50th and 97.5th percentiles of the predictions (*black solid lines*) were plotted with the 95% confidence interval (shaded areas).

To investigate appropriateness of selected covariates of the final result, the relationship between ANC profile and sex (**Figure 4**), DM (**Figure 5**) and age (**Figure 6**) was explored using raw data. In addition, the relationship between DM and covariate and treatment cycle distributions was also explored (**Table 6-8**), which was performed to see any clue in data supporting the modeling result that DM has protective effect on chemotherapy-induced myelosuppression. According to the data, women (**Figure 4**) and patients with no DM (**Figure 5**) were susceptible to chemotherapy induced neutropenia and older patients (over 60 yrs) with no DM were vulnerable to chemotherapy induced neutropenia (**Figure 6**), indicating the appropriateness of the selected covariates and the modeling result of protective effect of DM. However, there were significant differences in age, weight and BSA distributions between DM and non-DM groups, which might have influenced covariate selection process (**Table 6**).

**Table 9** investigated such possibility by incorporating age and BSA into $KDE_p$, which was significantly influenced by DM in the final model originally selected (**Table 5**). However, the results show that none of the 2 covariates significantly influenced $KDE_p$, indicating the original choice of DM was appropriate.

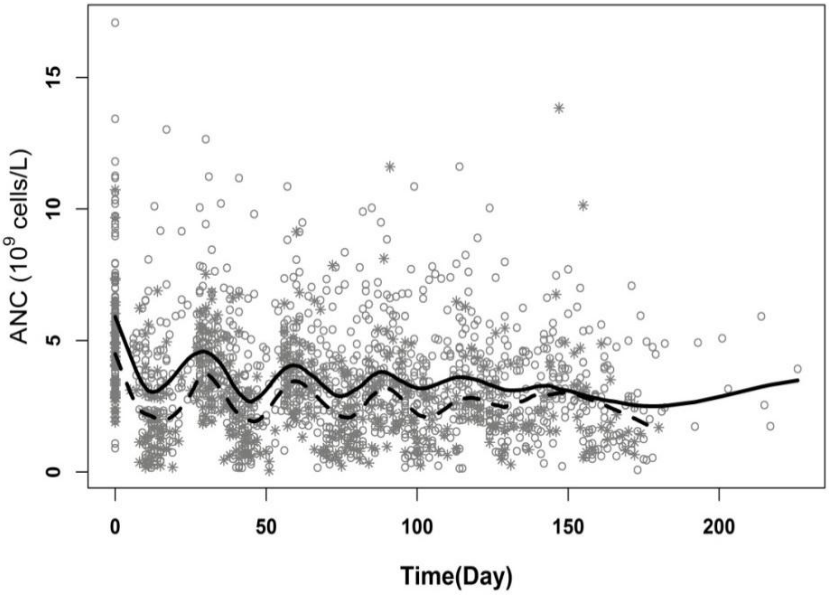


**Figure 4. Observed ANC vs. time plot for men** (circle: data, solid line: smooth) **and women** (asterisk: data, dashed line: smooth).

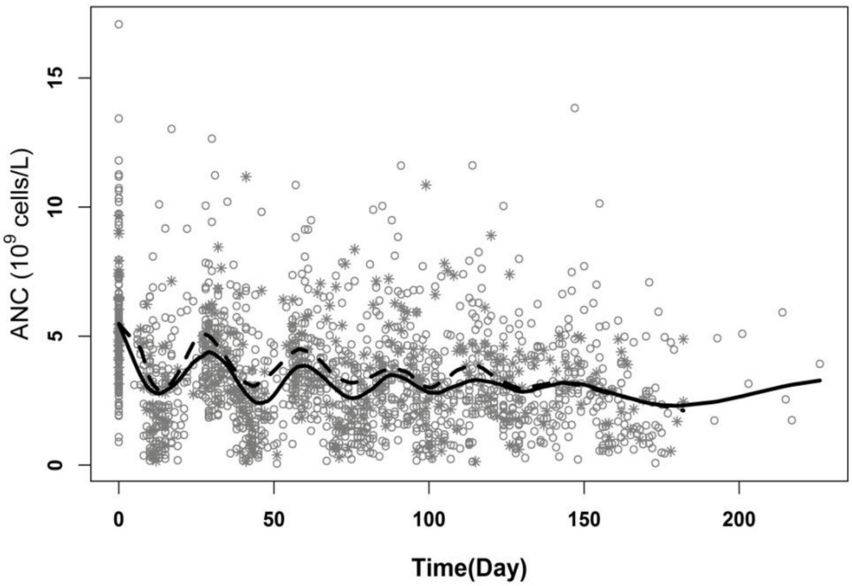


**Figure 5. Observed ANC vs. time plot for patients without DM** (circle: data, solid line: smooth) **and with DM** (asterisk: data, dashed line: smooth)**.**

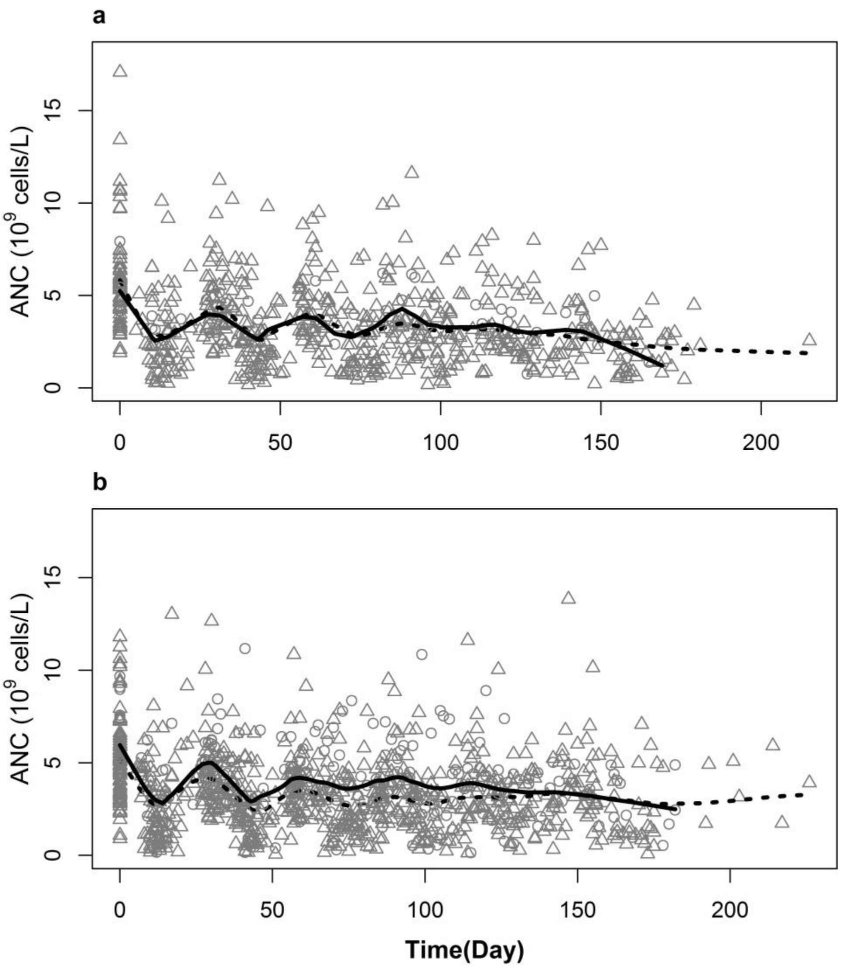


**Figure 6. Observed ANC vs. time plot for (a) patients under 60 years and (b) patients over 60 years, with non-DM** (triangle: data, dashed line: smooth) **and DM patients** (circle: data, solid line: smooth) **plotted together.**

**Table 6**. **Mean values of continuous covariates for non-DM (n=141) and DM patients (n=32)**

| | Non-DM patients | DM patients | P-value† |
|---|---|---|---|
| **Age (yrs)** | 60.2 | 64.5 | 0.0038* |
| **Weight (kg)** | 62.5 | 68.1 | 0.0133* |
| **Height (cm)** | 164.1 | 165.3 | 0.4660 |
| **BSA ($m^2$)** | 1.68 | 1.76 | 0.0170* |
| **ALT (IU/L)** | 20.1 | 25.0 | 0.2330 |
| **AST (IU/L)** | 21.1 | 22.7 | 0.6423 |
| **Creatinine (mg/dL)** | 0.84 | 0.93 | 0.0429 |
| **cCLcr (mL/min)** | 81.8 | 77.7 | 0.3622 |
| **eGFR (mL/min/1.73 $m^2$)** | 83.6 | 81.3 | 0.2361 |

†Independent t-test

*Significant P value

**Table 7. Categorical covariates for non-DM and DM patients**

| | Non-DM patients | DM patients | | Non-DM patients | DM patients |
|---|---|---|---|---|---|
| **ECOG PS, n (%)** | **$P^{\ddagger}$ = 1.0000** | | **Sex, n (%)** | **$P^{\ddagger}$=0.3733** | |
| 0 | 121 (69.9) | 28 (16.2) | Men | 101 (58.4) | 26 (15.0) |
| 1 | 20 (11.6) | 4 (2.3) | Women | 40 (23.1) | 6 (3.5) |
| **Stage, n (%)** | **$P^{\ddagger}$ =1.0000** | | **HTN, n (%)** | **$P^{\ddagger}$=0.0613** | |
| IIIB | 35 (20.2) | 8 (4.6) | No | 77 (37.4) | 11 (5.3) |
| IV | 106 (61.3) | 24 (13.9) | Yes | 64 (31.1) | 54 (26.2) |
| **Histology, n (%)** | **$P^{\ddagger}$=0.6118** | | **Pulmonary Tbc, n (%)** | **$P^{\ddagger}$= 0.3327** | |
| Adenoca. | 97 (56.1) | 22 (12.7) | No | 126 (72.8) | 26 (15.0) |
| Squamous | 40 (23.1) | 10 (5.8) | Yes | 15 (8.7) | 6 (3.5) |
| Unspecified | 4 (2.3) | 0 (0.0) | **Smoker, n (%)** | **$P^{\ddagger}$=0.3327** | |
| **Overall response, n (%)** | **$P^{\ddagger}$=0.4429** | | Non | 45 (26.0) | 6 (3.5) |
| PR | 34 (19.7) | 11 (6.4) | Current | 57 (32.9) | 15 (8.7) |
| SD | 45 (26.0) | 10 (5.8) | Ex | 39 (22.5) | 11 (6.4) |
| PD | 62 (35.8) | 11 (6.4) | | | |

‡ Chi-square test

**Table 8. Treatment cycles for non-DM and DM patients**

| No. of cycles | Non-DM (141) | DM (32) | P-value‡ |
|---|---|---|---|
| 2 | 7 (5%) | 1 (3%) | |
| 3 | 31 (22%) | 6 (19%) | |
| 4 | 21 (15%) | 6 (19%) | 0.9614 |
| 5 | 10 (7%) | 2 (6%) | |
| 6 | 72 (51%) | 17 (53%) | |

‡ Chi-square test

**Table 9. Covariate substitution Age or BSA on $KDE_p$ instead of DM on $KDE_p$ from the final model**

| Covariate | $OFV_{BEFORE}$ | $OFV_{AFTER}$ | ΔOFV | Criterion | d.f. | P-value |
|---|---|---|---|---|---|---|
| AGE on $KDE_p$ | 2878.92 | 2878.92 | 0.0001 | > 6.63 | 1 | 0.9748 |
| BSA on $KDE_p$ | 2878.92 | 2878.94 | -0.03 | > 6.63 | 1 | 0.8744 |

$KDE_p$ : *KDE* of paclitaxel

$OFV_{BEFORE}$ : OFV before covariate is added

$OFV_{AFTER}$ : OFV after covariate is added

d.f.: Degree of freedom

## IV. DISCUSSION

The model developed by Friberg et al.[14] has been applied to describe chemotherapy induced neutropenia. While most articles do not mention grade 4 neutropenia, it commonly occurs during anticancer treatment. Therefore, for the clinical setting, it would be important to be prepared for such severe neutropenia.

Ramon-Lopez et al.[39] developed the myelosuppression model including the effect of peripheral blood stem-cells transplantation and G-CSF treatment but this model did not use PK data. The KPD model used in this work has been successfully used for PD analyses in drug development when concentration data was not available.[38,39,45,46] Similarly in this work, the KPD model was used to describe treatment data for not only anticancer drugs but also G-CSF and therefore we expected ANC change after chemotherapy to be described more adequately.

Nevertheless, the information provided in this study is limited in that concentration information was not used and on the average only 2 observations per cycle were available for ANC outcome analysis. The limited number of data points might be the reason of poor precision for G-CSF related parameters. Myelosuppression model used in this work, however, was validated from previous studies, and therefore despite the limited information, we expect the result obtained would be applicable based on reasonable %RSE, acceptable GOF and VPC plots.

Among the selected covariates, women were reported to have higher risk for febrile neutropenia than men,[47] but there is little evidence that DM has protective effect on chemotherapy-induced myelosuppression. DM patients are rather known to have impaired mobilization of hematopoietic stem cells.[48,49] In our data, however, non-DM patients as well as women were observed to be more susceptible to the chemotherapy-induced neutropenia, which was consistent with the trend observed in the data as shown in **Figure 4** and **Figure 5**, indicating the selected covariates were appropriate based on the trend observed in the data.

Nevertheless, the possbility of confounding factors that could influence the selection of covariates was explored. One possibility considered was antidiabetic drugs or concomittent diseases that could influence the selection of DM. Metformin, one of the most frequently used antidiabetic drugs, was taken by 30 patients among DM group in this work and could impact on selecting DM. However, it is known that metformin inhibits differentiation of bone marrow stem cells via antimetabolitic effect.[50] Therefore, it would be unlikely that metformin can explain why DM patients showed less neutropenia than non DM patients. Other possibilities are age, weight and BSA, which were observed to be statistically significantly different between non-DM and DM patients ($P < 0.05$ as shown in **Tables 6-8**, indicating these covariates could be poential confounding factors for selectring DM. Among these 3 covariates, age was found to be most significantly different ($P = 0.0038$), which appears to be the most relavant risk factor to neutropenia. **Figure 6** shows ANC profiles of DM and non DM patients by dividing them into patients under 60 yrs (a: upper panel) and those over 60 yrs (b: lower panel). Younger patients showed no difference between DM and non DM groups but older patients with DM were resistant to chemotherapy induced neutropenia than older patients without DM. It is conjectured that this result might be related to the difference in body weight, which was observed to be significantly heavier in DM patients ($P = 0.0127$), suggesting a possibilty of more tolerance in obese people to chemotherapy induced neutropenia. To find out the possibility of age and BSA as the confounding factor of DM, each of age and BSA was incorporated into $KDE_p$ after DM effect was excluded from the model. However, none of the 2 covariates significantly improved the model. (**Table 9**) Therefore, DM was finally decided to be included into the final model. However, as the influence of DM on ANC change found in this work lacks physiological basis, more stuides inclusing external validatation would be needed to confirm this result.

Clinically, the proposed model can be used to predict the time to nadir ANC for a particular group of patients (for this model, sex and DM) and decide when G-CSF treatment should be involved and how to change dose regimen when it occurs, thereby avoiding serious risk in the immune system caused by severe neutropenia. That is, model-based simulation can be undertaken to explore the ANC time course according to patient characteristics for the treatment of G-CSF as shown in **Figure 7**, which shows the model can predict the ANC response based on the sex and DM.

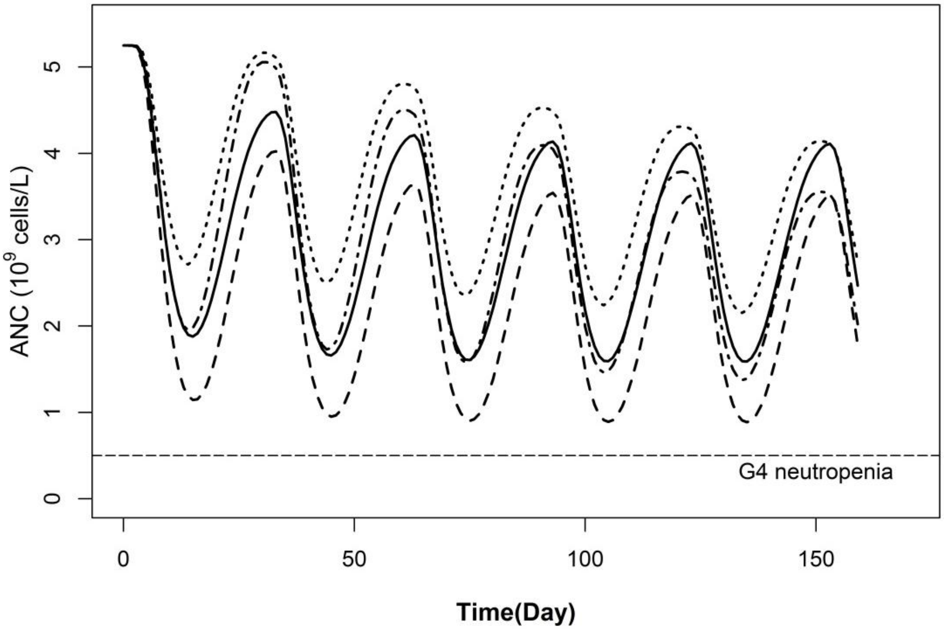


**Figure 7. Simulation result for the final model having the covariates of Sex and DM when the combination treatment of paclitaxel 297.5 mg/1.7 m$^2$ and cisplatin 127.5 mg/1.7 m$^2$ was given to the study patients with mean BSA of 1.7 m$^2$; men without DM** (*solid line*), **men with DM** (*dotted line*), **women without DM** (*dashed line*) **and women with DM** (*dashed and dotted line*). **The horizontal line indicates the grade 4 neutropenia (< 0.5 x10$^6$ cells/L).**

The final model developed in this work can be implemented in a web based program. **Figure 8** shows the simulated result based on R and the shiny package,[51] which enables chemotherapy dose adjustment according to BSA: paclitaxel 175 mg/m$^2$ and cisplatin 75 mg/m$^2$ and patient covariates of sex and concomitant DM.

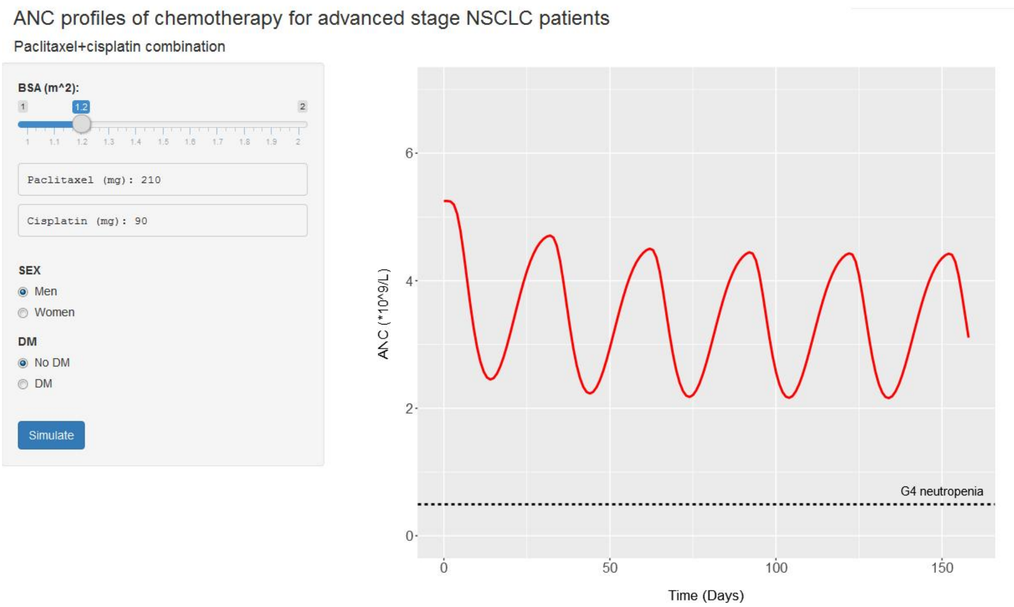


**Figure 8. Interactive pharmacometric application developed using Shiny for the R programming language, illustrating dose adjustment in chemotherapy according to BSA**: paclitaxel 175 mg/m$^2$ and cisplatin 75 mg/m$^2$ and patient covariates of sex and concomitant DM. This program is uploaded in the web page: http://neutropenia-2016.shinyapps.io/Shiny/.

In addition, the model can be extended to suggesting the optimal dose to avoid neutropenia induced by chemotherapy. However, changing chemotherapy dose could be risky from the aspect of maintaining the efficacy of a drug. At this point, the efficacy of chemotherapy was not considered in this model. However, if the model that can handle both efficacy and toxicity can be developed, it would be able to predict the time to increase or decrease the dose of chemotherapy to maximize the efficacy and minimize the toxicity, thereby optimizing the treatment outcome over the entire course of chemotherapy.

## V. CONCLUSION

In conclusion, despite limitations mentioned above, the present approach is considered to be valuable to enhancing the quantitative understanding of neutropenia induced by chemotherapy, and we propose it as an alternative tool for evaluating and comparing adverse events of various chemotherapy drugs.

## REFERENCE

1. Prevalence rate and five year survival rate of neoplasms in Korea. Available at http://kosis.kr/statHtml/statHtml.do?orgId=117&tblId=DT_117N_A00021&conn_path=I3 [Accessed 12/May 2014]

2. Cause of death in Korea 2013. Available at http://kosis.kr/statisticsList/statisticsList_01List.jsp?vwcd=MT_ZTITLE&parmTabId=M_01_01#SubCont [Accessed 18/Dec 2014]

3. Horn L, Pao W, H. JD. Neoplasms of the lung. In: Longo DL, Fauci AS, Kasper DL, Hauser SL, Jameson JL, Loscalzo J, editors. Harrison's Principles of Internal Medicine. 18th ed. New York, NY: McGraw-Hill; 2012.

4. Delbaldo C, Michiels S, Rolland E, Syz N, Soria JC, Le Chevalier T, et al. Second or third additional chemotherapy drug for non-small cell lung cancer in patients with advanced disease. Cochrane Database Syst Rev 2007:CD004569.

5. Azzoli CG, Temin S, Giaccone G. 2011 Focused Update of 2009 American Society of Clinical Oncology Clinical Practice Guideline Update on Chemotherapy for Stage IV Non-Small-Cell Lung Cancer. J Oncol Pract 2012;8:63-6.

6. Lilenbaum RC, Langenberg P, Dickersin K. Single agent versus combination chemotherapy in patients with advanced nonsmall cell lung carcinoma: a meta-analysis of response, toxicity, and survival. Cancer 1998;82:116-26.

7. Johnson ML, Patel JD. Chemotherapy and targeted therapeutics as maintenance of response in advanced non-small cell lung cancer. Semin Oncol 2014;41:93-100.

8. Ettinger DS. Non-small cell lung cancer treatment-related bone marrow

toxicities. Semin Oncol 2005;32:S81-5.

9. Schiller JH, Harrington D, Belani CP, Langer C, Sandler A, Krook J, et al. Comparison of four chemotherapy regimens for advanced non-small-cell lung cancer. N Engl J Med 2002;346:92-8.

10. Kroep JR, Smit EF, Giaccone G, Van der Born K, Beijnen JH, Van Groeningen CJ, et al. Pharmacology of the paclitaxel-cisplatin, gemcitabine-cisplatin, and paclitaxel-gemcitabine combinations in patients with advanced non-small cell lung cancer. Cancer Chemother Pharmacol 2006;58:509-16.

11. Bodey GP. Citation Classic - Quantitative Relationships between Circulating Leukocytes and Infection in Patients with Acute-Leukemia. Current Contents/Clinical Practice 1981:28.

12. Freifeld AG, Bow EJ, Sepkowitz KA, Boeckh MJ, Ito JI, Mullen CA, et al. Clinical Practice Guideline for the Use of Antimicrobial Agents in Neutropenic Patients with Cancer: 2010 Update by the Infectious Diseases Society of America. Clinical Infectious Diseases 2011;52:E56-E93.

13. Lyman GH, Michels SL, Reynolds MW, Barron R, Tomic KS, Yu J. Risk of mortality in patients with cancer who experience febrile neutropenia. Cancer 2010;116:5555-63.

14. Friberg LE, Henningsson A, Maas H, Nguyen L, Karlsson MO. Model of chemotherapy-induced myelosuppression with parameter consistency across drugs. J Clin Oncol 2002;20:4713-21.

15. Joerger M, Huitema AD, van den Bongard DH, Schellens JH, Beijnen JH. Quantitative effect of gender, age, liver function, and body size on the population pharmacokinetics of Paclitaxel in patients with solid tumors. Clin Cancer Res 2006;12:2150-7.

16. Kloft C, Wallin J, Henningsson A, Chatelut E, Karlsson MO. Population pharmacokinetic-pharmacodynamic model for neutropenia with patient subgroup identification: comparison across anticancer drugs. Clin Cancer Res 2006;12:5481-90.

17. Latz JE, Karlsson MO, Rusthoven JJ, Ghosh A, Johnson RD. A semimechanistic-physiologic population pharmacokinetic/pharmacodynamic model for neutropenia following pemetrexed therapy. Cancer Chemother Pharmacol 2006;57:412-26.

18. Ozawa K, Minami H, Sato H. Population pharmacokinetic and pharmacodynamic analysis for time courses of docetaxel-induced neutropenia in Japanese cancer patients. Cancer Sci 2007;98:1985-92.

19. Puisset F, Alexandre J, Treluyer JM, Raoul V, Roche H, Goldwasser F, et al. Clinical pharmacodynamic factors in docetaxel toxicity. Br J Cancer 2007;97:290-6.

20. Hing J, Perez-Ruixo JJ, Stuyckens K, Soto-Matos A, Lopez-Lazaro L, Zannikos P. Mechanism-based pharmacokinetic/pharmacodynamic meta-analysis of trabectedin (ET-743, Yondelis) induced neutropenia. Clin Pharmacol Ther 2008;83:130-43.

21. Schmitt A, Gladieff L, Laffont CM, Evrard A, Boyer JC, Lansiaux A, et al. Factors for hematopoietic toxicity of carboplatin: refining the targeting of carboplatin systemic exposure. J Clin Oncol 2010;28:4568-74.

22. van Hasselt JG, Gupta A, Hussein Z, Beijnen JH, Schellens JH, Huitema AD. Population pharmacokinetic-pharmacodynamic analysis for eribulin mesilate-associated neutropenia. Br J Clin Pharmacol 2013;76:412-24.

23. Joerger M, Huitema AD, Richel DJ, Dittrich C, Pavlidis N, Briasoulis E, et al.

Population pharmacokinetics and pharmacodynamics of paclitaxel and carboplatin in ovarian cancer patients: a study by the European organization for research and treatment of cancer-pharmacology and molecular mechanisms group and new drug development group. Clin Cancer Res 2007;13:6410-8.

24. Leger F, Loos WJ, Bugat R, Mathijssen RH, Goffinet M, Verweij J, et al. Mechanism-based models for topotecan-induced neutropenia. Clin Pharmacol Ther 2004;76:567-78.

25. Zandvliet AS, Schellens JH, Dittrich C, Wanders J, Beijnen JH, Huitema AD. Population pharmacokinetic and pharmacodynamic analysis to support treatment optimization of combination chemotherapy with indisulam and carboplatin. Br J Clin Pharmacol 2008;66:485-97.

26. van Kesteren C, Zandvliet AS, Karlsson MO, Mathot RA, Punt CJ, Armand JP, et al. Semi-physiological model describing the hematological toxicity of the anti-cancer agent indisulam. Invest New Drugs 2005;23:225-34.

27. Kathman SJ, Williams DH, Hodge JP, Dar M. A Bayesian population PK-PD model of ispinesib-induced myelosuppression. Clin Pharmacol Ther 2007;81:88-94.

28. Panetta JC, Schaiquevich P, Santana VM, Stewart CF. Using pharmacokinetic and pharmacodynamic modeling and simulation to evaluate importance of schedule in topotecan therapy for pediatric neuroblastoma. Clin Cancer Res 2008;14:318-25.

29. Soto E, Staab A, Tillmann C, Trommeshauser D, Fritsch H, Munzert G, et al. Semi-mechanistic population pharmacokinetic/pharmacodynamic model for neutropenia following therapy with the Plk-1 inhibitor BI 2536 and its application in clinical development. Cancer Chemother Pharmacol

2010;66:785-95.

30. Joerger M, Kraff S, Huitema AD, Feiss G, Moritz B, Schellens JH, et al. Evaluation of a pharmacology-driven dosing algorithm of 3-weekly paclitaxel using therapeutic drug monitoring: a pharmacokinetic-pharmacodynamic simulation study. Clin Pharmacokinet 2012;51:607-17.

31. Hansson EK, Friberg LE. The shape of the myelosuppression time profile is related to the probability of developing neutropenic fever in patients with docetaxel-induced grade IV neutropenia. Cancer Chemother Pharmacol 2012;69:881-90.

32. Vainas O, Ariad S, Amir O, Mermershtain W, Vainstein V, Kleiman M, et al. Personalising docetaxel and G-CSF schedules in cancer patients by a clinically validated computational model. Br J Cancer 2012;107:814-22.

33. Pastor ML, Laffont CM, Gladieff L, Schmitt A, Chatelut E, Concordet D. Model-based approach to describe G-CSF effects in carboplatin-treated cancer patients. Pharm Res 2013;30:2795-807.

34. Common Terminology Criteria for Adverse Events v3.0 (CTCAE). Available at http://ctep.cancer.gov/protocolDevelopment/electronic_applications/docs/ctcaev3.pdf [Accessed 05 February 2016]

35. Cockcroft DW, Gault MH. Prediction of creatinine clearance from serum creatinine. Nephron 1976;16:31-41.

36. Twomey PJ, Reynolds TM. The MDRD formula and validation. Qjm 2006;99:804-5.

37. Kallner A, Ayling PA, Khatami Z. Does eGFR improve the diagnostic capability of S-Creatinine concentration results? A retrospective population

based study. Int J Med Sci 2008;5:9-17.

38. Jacqmin P, Snoeck E, van Schaick EA, Gieschke R, Pillai P, Steimer JL, et al. Modelling response time profiles in the absence of drug concentrations: definition and performance evaluation of the K-PD model. J Pharmacokinet Pharmacodyn 2007;34:57-85.

39. Ramon-Lopez A, Nalda-Molina R, Valenzuela B, Perez-Ruixo JJ. Semi-mechanistic model for neutropenia after high dose of chemotherapy in breast cancer patients. Pharm Res 2009;26:1952-62.

40. Minto CF, Schnider TW, Short TG, Gregg KM, Gentilini A, Shafer SL. Response surface model for anesthetic drug interactions. Anesthesiology 2000;92:1603-16.

41. Sandstrom M, Lindman H, Nygren P, Johansson M, Bergh J, Karlsson MO. Population analysis of the pharmacokinetics and the haematological toxicity of the fluorouracil-epirubicin-cyclophosphamide regimen in breast cancer patients. Cancer Chemother Pharmacol 2006;58:143-56.

42. Bauer RJ. Introduction to NONMEM 7.3.0. NONMEM user guide. Hanover, MD 21076: ICON Development Solutions; 2013. p.209.

43. Lindbom L, Ribbing J, Jonsson EN. Perl-speaks-NONMEM (PsN)--a Perl module for NONMEM related programming. Comput Methods Programs Biomed 2004;75:85-94.

44. Lindbom L, Pihlgren P, Jonsson EN. PsN-Toolkit--a collection of computer intensive statistical methods for non-linear mixed effect modeling using NONMEM. Comput Methods Programs Biomed 2005;79:241-57.

45. Romberg R, Olofsen E, Sarton E, Teppema L, Dahan A. Pharmacodynamic effect of morphine-6-glucuronide versus morphine on hypoxic and

hypercapnic breathing in healthy volunteers. Anesthesiology 2003;99:788-98.

46. Pillai G, Gieschke R, Goggin T, Jacqmin P, Schimmer RC, Steimer JL. A semimechanistic and mechanistic population PK-PD model for biomarker response to ibandronate, a new bisphosphonate for the treatment of osteoporosis. Br J Clin Pharmacol 2004;58:618-31.

47. Crawford J, Glaspy JA, Stoller RG, Tomita DK, Vincent ME, McGuire BW, et al. Final Results of a Placebo-Controlled Study of Filgrastim in Small-Cell Lung Cancer: Exploration of Risk Factors for Febrile Neutropenia. Supportive Cancer Therapy 2005;3:36-46.

48. Fadini GP, Albiero M, Vigili de Kreutzenberg S, Boscaro E, Cappellari R, Marescotti M, et al. Diabetes impairs stem cell and proangiogenic cell mobilization in humans. Diabetes Care 2013;36:943-9.

49. Ferraro F, Lymperi S, Mendez-Ferrer S, Saez B, Spencer JA, Yeap BY, et al. Diabetes impairs hematopoietic stem cell mobilization by altering niche function. Sci Transl Med 2011;3:104ra1.

50. Liu X, Zheng H, Yu WM, Cooper TM, Bunting KD, Qu CK. Maintenance of mouse hematopoietic stem cells ex vivo by reprogramming cellular metabolism. Blood 2015;125:1562-5.

51. Wojciechowski J, Hopkins AM, Upton RN. Interactive Pharmacometric Applications Using R and the Shiny Package. CPT Pharmacometrics Syst Pharmacol 2015;4:e00021.

**ABSTRACT (IN KOREAN)**

비소세포폐암환자에서 항암치료에 의한 골수억제를 최소화할 수 있는 모형 기반 최적 용량 요법 디자인 계획의 개발

<지도교수 박 경 수>

연세대학교 대학원 의과학과

김 유 경

폐암은 진행된 상태로 발견되는 경우가 흔하고 그러므로 항암요법이 중요한 치료 중 하나이다. 폐암 4기 환자는 보통 2개 이상의 항암제로 복합치료를 받게 된다. 골수억제는 항암치료 받는 암환자에서 가장 흔하게 발생할 수 있는 부작용 중 하나로 항암치료 효율이 감소하며 감염성 질환에 걸릴 위험성을 증가시킨다. 현재 항암제 치료용량 결정은 체질량지수로 결정하고 있으나 그에 따른 환자반응은 다양하게 나타난다. 그러므로 본 연구의 목적은 비소세포폐암 환자에서 항암치료에 의한 골수억제를 최소화 할 수 있는 모형 기반 최적 용량 요법 계획의 개발이다.

항암치료시 시간에 따른 절대중성구수(absolute neutrophil count;ANC) 변화를 표현하기 위해 반생리적 모형(semi-mechanistic model)이 사용되었다. 또한 약물의 혈중농도값이 없으므로 이를 대신할 수 있는 동력-약력학 모형(kinetic-pharmacodynamic model)을 가상의 구획을 이용하여 표

현하였다. 반생리적 모형은 중성구 생산 구획, 세 개의 중성구 성숙 구획, 혈액 내 중성구를 나타내는 구획으로 표현되며 중성구 생산은 혈액 내 음성 피드백에 의해 영향을 받고 항암치료에 의해 감소한다고 가정하였다.

최종 구조 모형은 반응 표면 모형(response surface model)으로 파클리탁셀과 시스플라틴의 복합치료 효과를 표현하고, G-CSF는 보통 최대효과 모형(ordinary Emax model)으로 표현한 반생리적 모형이다. 공변량 모형은 50%의 최대 약물 억제 반응을 나타내는 가상의 용량 속도인 $IR_{50,drug}$에서 여성의 경우 38% 감소하고, 파클리탁셀의 가상 구획에서 효과처로의 제거속도인 $KDE_{paclitaxel}$은 당뇨 환자에서 85% 감소하였다. 이 결과가 관찰 데이터에서 보이는 경향성과 일치함에도 불구하고 위의 공변량과 ANC 간의 생리적 관계가 부족하기 때문에 이 결과를 확신하기 위해 외부검정과정을 포함한 좀더 많은 연구가 필요하다. 모형은 파라미터 추정치의 정확도, goodness of fit, visual predictive check 와 같은 진단 그림을 통해 평가하였고 최종 모델은 수집된 데이터를 좋은 정확도로 잘 설명한다고 볼 수 있다. 임상적으로 최종적으로 제안된 모형은 과립세포군 촉진인자가 필요한 최저 절대중성구수가 언제 발생할지 예측하고 발생한 후 어떻게 용량을 조절해야 하는 지를 예측하여 중증 중성구감소증에 의한 위험을 감소시키는 데 도움이 될 수 있다.

핵심되는 말: 중성구감소증, 정량적 분석방법, 비소세포폐암, 파클리탁셀, 시스플라틴, 반생리적 골수억제 모형, 동력-약력학 모형, 반응 표면 모형, 이행구획 모형, 일상적 임상자료